Positioning Controller of a Remotely Operated Vehicle Using RWNN-based Adaptive Robust Controllers

Guoqing Xia, Chengcheng Pang, Ju Liu, Jingjing, Xue
College of Automation
Harbin Engineering University
Harbin, China
xiaguoqing@hrbeu.edu.cn, pcc_mail@163.com , xuejingjing@hrbeu.edu.cn

***Abstract*—In this paper, a robust adaptive controller is designed for the dynamical positioning of a remotely operated vehicle (ROV) with unknown hydrodynamic coefficients and disturbances. Firstly, the Multiple Input Multiple Output (MIMO) system can be divided into several Single Input Single Output (SISO) systems for convenience of controller design. Then, a recurrent wavelet neural network (RWNN) with feedback loops is employed to approach the unknown part of the controller, and it can greatly reduce the number of neural network's inputs. Though the upper bounds of the network's approximation errors and disturbances are often used in the existed work, they are not necessary in this paper by presenting a special robust compensator. The stability analysis is given by Lyapunov theorem, and the tracking errors are proved to convergence to zero. Simulation result are presented for the ROV's positioning system, which indicate that the proposed controller has a good performance.**

***Keywords*—recurrent wavelet neural network, underwater vehicle, dynamic positioning, adaptive control**

I. Introduction

Underwater vehicles have been widely used in some marine missions for a long time, such as marine science, submarine rescue, data gathering, and so on. For some specific tasks, it is required that the vehicles keep their position close to some structures precisely [1, 2]. So 6-DOF dynamic positioning controllers are necessary for these situations. In view of the 6-DOF control issues, the design of controllers face a lot of troubles because of the existence of strong coupling character, nonlinear nature, unknown parameters and unknown disturbances. Therefore, it is a significant and challenging task for designing a 6-DOF controller with the ability to cope with these factors.

Many researchers have made a lot of work on the control issues of underwater vehicles. Fossen gave a comprehensive introduction of the marine vehicles systems including modeling, guidance, navigation and control [3]. Mode-based controllers are often utilized in underwater vehicle systems. Lyapunov method, backstepping method, feedback linearization and some combined methods are widely used in this field [4,5]. However, most of these controllers require the accurate mathematical model of the vehicle, which is often difficult to obtain in practice. Adaptive controllers are developed in many studies to overcome these problems by estimating the unknown slowly varying parameters [6,7]. An adaptive PD controller for 4-DOF positioning of a ROV is discussed to keep the ROV's position close to an underwater structure. The disturbing force caused by ocean current, passive arms, and umbilical cables had been compensated by adaptive estimation [8]. In [9], the researchers proposed a MIMO nonlinear adaptive robust controller, with the unknown hydrodynamic parameters of the vehicle and the slowly varying disturbances were estimated.

Approximation-based control methods such as neural networks and fuzzy logic system are also effective tools to overcome the limitations of the controller mentioned above. It is usually utilized to deal with the unknown term, nonlinear terms or time-varying disturbance in vehicles' dynamic system. In [10, 11], the authors described an efficient fuzzy controller, which reduced the conventional two-input fuzzy controller to a single input fuzzy controller. The main advantage in this approach is that rule inferences are now greatly reduced and the calculation procedure is simplified. In [12], the vehicle's dynamic uncertainties are approximated by utilizing a single hidden layered neural network. In [13], researchers present a semi-globally stable adaptive controller for diving control of an Autonomous Underwater Vehicle(AUV), and the unknown terms in pitch a neural network compensates motion. An adaptive output feedback controller for AUV is proposed in [14], and a recurrent fuzzy neural network (DRFNN) is employed to estimate the dynamic uncertain nonlinear mapping. And in this paper, a robust controller is designed for compensate the external disturbances and unknown network's approximation errors.

Wavelet neural network (WNN) has the advantages in its dynamic responses and information storing ability [15, 16]. A WNN-based adaptive robust controller is investigated to resolve the MIMO tracking control system [15]. By the further study, in [16], a recurrent wavelet neural backstepping control (RWNBC) scheme including a neural network and a smooth compensator is developed for MIMO systems. Since there is an internal feedback loop in it, the RWNN can capture the dynamics of a system, so the number of inputs of RWNN is less than the conventional neural network. So in this paper, a

RWNN will be used to approach the unknown part in the ideal controller, which includes the uncertain parameters of the vehicles.

In current studies, the common problems of the existing methods of underwater vehicles are as follows: a) AUV controllers are usually designed according to the three degrees of freedom motion. Six-DOF control issue is more complicated and has more challenge; b) The transform matrix' derivation is used in many controllers, which is very complex and the derivation of the six-DOF motion system is difficult to obtain; c) In some researches, robust terms are used to suppress or offset the effect of jamming, and the upper limits of the disturbances are necessary customarily. d) Most controllers can ensure that the tracking error converge to a neighborhood of zero, which cannot satisfy the precision demands.

The main contribution of this paper is to propose a RWNN-based adaptive robust controller for the six-DOF dynamic system of underwater vehicles subject to unknown external disturbances, model uncertainties and strong coupling. A RWNN is used to approach the unknown terms, so the designed controller can be close to the ideal controller. Besides, a special robust term is developed to handle the neural network's approximation error and equivalent disturbances.

The structure of this paper is organized as follows. Section II states the control problem of underwater vehicles subject to uncertain terms and disturbances. Section III presents the design of the WRNN-based controller and a robust compensator. In section IV, simulation studies are shown to verify the effectiveness of the proposed control scheme. Finally, conclusions are made in the last section.

II. PROBLEM FORMULATION

To analyze the dynamic behavior of the ROV and the effect of the umbilical cable, three coordinate systems are defined below (see Fig 1), i.e. body-fixed frame, earth-fixed frame and the local frames along the cable.

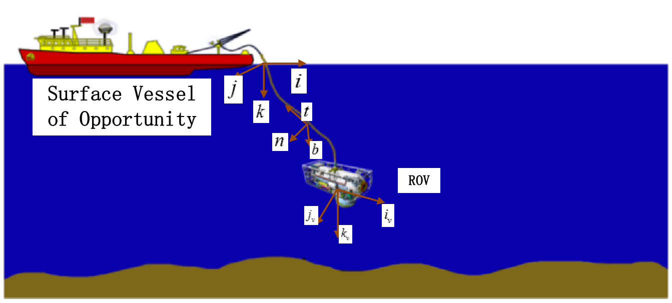

Fig. 1. Coordinate systems of the ROV system

The body-fixed frame $(\mathbf{o-xyz})$ is attached to the ROV, and $(\mathbf{i_v}, \mathbf{j_v}, \mathbf{k_v})$ is the unit vector. The earth-fixed frame $(\mathbf{O-XYZ})$ is selected at the ocean surface and the unit vector is defined as $(\mathbf{i}, \mathbf{j}, \mathbf{k})$. In addition, local fames $(\mathbf{tnb})$ are employed to study the disturbance caused by umbilical cable, and the local frames are located at the points along the cable with $\mathbf{t}$ tangent to the cable in the direction of increasing arc length from the tow-point, and $\mathbf{n}$ is the normal vector, $\mathbf{b}$ is in the plane of $(\mathbf{i}, \mathbf{j})$.

The relationship between the three frames can be expressed as:

$$\begin{aligned} [\boldsymbol{i}_v \quad \boldsymbol{j}_v \quad \boldsymbol{k}_v] &= [\boldsymbol{i} \quad \boldsymbol{j} \quad \boldsymbol{k}]\mathbf{J}_1(\phi, \theta, \psi) \\ [\boldsymbol{t} \quad \boldsymbol{n} \quad \boldsymbol{b}] &= [\boldsymbol{i} \quad \boldsymbol{j} \quad \boldsymbol{k}]\mathbf{W}(\alpha, \beta) \end{aligned} \tag{1}$$

where $\mathbf{J}_1(\phi, \theta, \psi)$ is the transformation matrix and the Euler rotation angers ϕ, θ, ψ stand for roll, pitch and heading angles of the ROV. α, β are local rotational angles.

A. ROV's mathematical description

The six-DOF mathematical model of ROV can be described by the following equations [13]:

$$\begin{aligned} &\dot{\boldsymbol{\eta}} = \mathbf{J}(\boldsymbol{\eta})\mathbf{v} \\ &\mathbf{M}\dot{\mathbf{v}} + \mathbf{C}(\mathbf{v})\mathbf{v} + \mathbf{D}(\mathbf{v})\mathbf{v} + \mathbf{G}(\boldsymbol{\eta}) = \boldsymbol{\tau} + \mathbf{J}^{-1}(\boldsymbol{\eta})\Delta f \\ &\mathbf{y} = \boldsymbol{\eta} \end{aligned} \tag{2}$$

where $\boldsymbol{\eta} = [x, y, z, \phi, \theta, \psi]^{\mathrm{T}} \in \Re^{6\times1}$ is the vehicle's position and attitude vector in six DOF in the earth-fixed frame; $\mathbf{v} = [u, v, w, p, q, r]^{\mathrm{T}} \in \Re^{6\times1}$ denote the linear velocities and angular velocities in body-fixed frame. The output vector $\mathbf{y} \in \Re^{6\times1}$ is measurable in the system. $\boldsymbol{\tau} \in \Re^{6\times1}$ is the input vector, which includes the forces and moments produced by thrusters. $\mathbf{M} = \mathbf{M_A} + \mathbf{M_{RB}}$ is the system inertial matrix (including added mass), $\mathbf{C}(\mathbf{v})$ is the Coriolis and centripetal matrix (including added mass), and $\mathbf{C}(\mathbf{v}) = \mathbf{C_A}(\mathbf{v}) + \mathbf{C_{RB}}(\mathbf{v}) \in \Re^{6\times6}$. The hydrodynamic damping matrix $\mathbf{D}(\mathbf{v}) \in \Re^{6\times6}$ can be divided into linear and nonlinear parts. $\mathbf{G}(\boldsymbol{\eta}) \in \Re^{6\times6}$ represents the restoring forces and moments. $\Delta f \in \Re^{6}$ is a vector of bias forces and moments and consist of slowly varying environmental disturbances, unmolded terms and the forces caused by the cable. $\mathbf{J}(\boldsymbol{\eta}) \in \Re^{6\times6}$ is the transformation matrix, and

$$\mathbf{J}(\boldsymbol{\eta}) = \begin{bmatrix} \mathbf{J}_1(\boldsymbol{\eta}) & \mathbf{0} \\ \mathbf{0} & \mathbf{J}_2(\boldsymbol{\eta}) \end{bmatrix} \tag{3}$$

where $\mathbf{J}_1(\boldsymbol{\eta})$ and $\mathbf{J}_2(\boldsymbol{\eta})$ are complex functions of $\Omega = [\phi, \theta, \psi]^{\mathrm{T}}$.

B. Dynamic Modeling of Umbilical Cable

The cable can be considered as a long, thin, elastic cylinder. Assumed that the cable can only sustain tensile loads. Defining the state vector[17,18]:

$$\boldsymbol{y} = [T \quad V_t \quad V_n \quad V_b \quad \alpha \quad \beta]^T \tag{4}$$

where T is the tension forces, and V_t 、 V_n 、 V_b are the components of the velocity vector V_c, which is the velocity term in the local frames along the umbilical cable. So the cable dynamics can be expressed by the following partial differential equation:

$$\mathbf{M}_{cable}\frac{\partial \boldsymbol{y}_{cab}}{\partial s_c} = \mathbf{N}_{cable}\frac{\partial \boldsymbol{y}_{cab}}{\partial t} + \mathbf{Q} \tag{5}$$

where

$$\mathbf{M}_{cable} = \begin{bmatrix} 1 & 0 & 0 & 0 & 0 & 0 & \\ 0 & 1 & 0 & 0 & V_b\cos\beta & -V_n & \\ 0 & 0 & 1 & 0 & -V_b\sin\beta & V_t & 0 \\ 0 & 0 & 0 & 1 & V_n\sin\beta - V_t\cos\beta & 0 & \\ 0 & 0 & 0 & 0 & -T\cos\beta & 0 & \\ 0 & 0 & 0 & 0 & 0 & T & \end{bmatrix}$$

$$\mathbf{Q} = \begin{bmatrix} W\sin\beta + \frac{1}{2}\pi\rho d\sqrt{1+eT}C_t\,\mathrm{U}_{r\_t}\left|\mathrm{U}_{r\_t}\right| \\ 0 \\ 0 \\ 0 \\ \frac{1}{2}\rho d\sqrt{1+eT}C_n\,\mathrm{U}_{r\_\mathrm{b}}\sqrt{\mathrm{U}_{r\_\mathrm{n}}^2 + \mathrm{U}_{r\_\mathrm{b}}^2} - \rho A\dot{\mathrm{U}}_{c\_\mathrm{b}} \\ W\cos\beta + \frac{1}{2}\rho d\sqrt{1+eT}C_n\,\mathrm{U}_{r\_\mathrm{n}}\sqrt{\mathrm{U}_{r\_\mathrm{n}}^2 + \mathrm{U}_{r\_\mathrm{b}}^2} - \rho A\dot{\mathrm{U}}_{c\_n} \end{bmatrix}$$

$$\mathbf{N}_{cable} = \begin{bmatrix} \frac{-meV_t}{1+eT} & m & 0 & 0 & (m_1V_b - \rho A\mathrm{U}_{c\_b})\cos\beta & -(m_1V_n - \rho A\mathrm{U}_{c\_n}) \\ e & 0 & 0 & 0 & 0 & 0 \\ 0 & 0 & 0 & 0 & 0 & 1+eT \\ 0 & 0 & 0 & 0 & -(1+eT)\cos\beta & 0 \\ \frac{-e(m_1V_b - \rho A\mathrm{U}_{c\_b})}{1+eT} & 0 & m_1 & m_1 & (m_1V_n - \rho A\mathrm{U}_{c\_n})\sin\beta - mV\cos\beta_t & 0 \\ \frac{-me(m_1V_n - \rho A\mathrm{U}_{c\_n})}{1+eT} & m_1 & 0 & 0 & -(m_1V_b - \rho A\mathrm{U}_{c\_b})\sin\beta & mV_t \end{bmatrix}$$

where s_c denotes the un-stretched arc length of the cable, $e = 1/EA$, and E is the Young's modulus. ρ is the fluid density (1025 kg/m^3 for seawater), m is the mass per unit length, and $m_1 = m + \rho A$ is the virtual mass per unit length, W denotes the weight per unit length of the cable, and $W = (m - \rho A)\mathrm{g}$, where g is the gravitational acceleration. $\mathrm{U}_c = [\mathrm{U}_{c\_t} \quad \mathrm{U}_{c\_n} \quad \mathrm{U}_{c\_b}]^{\mathrm{T}}$ is the velocity vector of the ocean current in the local frame. $\mathrm{U}_r = V_c - \mathrm{U}_c$ is the velocity relative to the current, and can be expressed as $\mathrm{U}_r = [\mathrm{U}_{r\_t} \quad \mathrm{U}_{r\_n} \quad \mathrm{U}_{r\_b}]^{\mathrm{T}}$ in the $\mathbf{tnb}$ frame.

The initial condition of the umbilical cable and six boundary conditions are needed to solve the partial differential equation (5). Assumption that the surface vessel is in the dynamic positioning mode, and that the influence of the cable by the heave movement can be neglected. So the boundary conditions can be expressed as:

$$\begin{aligned} &V_c(\mathrm{S},\mathrm{t}) = 0; \\ &V_c(0,\mathrm{t}) = \mathbf{W}^T(\alpha,\beta)\mathbf{J}_1(\phi,\theta,\psi)(\mathbf{v} + \Omega\times\boldsymbol{r}_c) \end{aligned} \tag{6}$$

The forces and moment caused by the tension of the umbilical cable are expressed by:

$$\mathbf{F}_c(t) = \begin{bmatrix} F_{cX} \\ F_{cY} \\ F_{cZ} \end{bmatrix} = R^T(\phi,\theta,\varphi)W(\alpha(0,t),\beta(0,t))\begin{bmatrix} T(0,t) \\ 0 \\ 0 \end{bmatrix} \tag{7}$$

$$\mathbf{M}_c(t) = \begin{bmatrix} M_{cX} \\ M_{cY} \\ M_{cZ} \end{bmatrix} = \boldsymbol{r}_c\times\mathbf{F}_c(t) = \begin{bmatrix} y_cF_{cZ} - z_cF_{cY} \\ z_cF_{cX} - x_cF_{cY} \\ x_cF_{cY} - y_cF_{cX} \end{bmatrix} \tag{8}$$

where . $\boldsymbol{r}_c = [x_c, y_c, z_c]^{\mathrm{T}}$ denote the position of the joint point in the body-fixed frame.

C. *Model for Controller Design*

Define $\mathbf{x} = \left[\boldsymbol{\eta}^{\mathrm{T}}, \dot{\boldsymbol{\eta}}^{\mathrm{T}}\right]^{\mathrm{T}}$, $\mathbf{y} = \boldsymbol{\eta} = \left[y_1, ..., y_n\right]^{\mathrm{T}}$, and the model (1) can be rewritten as:

$$\ddot{\mathbf{y}} = f(\mathbf{x}) + \mathbf{M}_{\boldsymbol{\eta}}^{-1}(\boldsymbol{\eta})\mathbf{u} + \mathbf{b}_{\boldsymbol{\eta}} \tag{9}$$

where

$$\begin{aligned} f(\mathbf{x}) &= -\mathbf{J}(\boldsymbol{\eta})\mathbf{M}^{-1}[\mathbf{C}(\mathbf{v}) - \mathbf{M}\mathbf{J}^{-1}(\boldsymbol{\eta})\dot{\mathbf{J}}(\boldsymbol{\eta})]\mathbf{J}^{-1}(\boldsymbol{\eta})\dot{\boldsymbol{\eta}} \\ &-\mathbf{J}(\boldsymbol{\eta})\mathbf{M}^{-1}\mathbf{D}(\mathbf{v})\mathbf{J}^{-1}(\boldsymbol{\eta})\dot{\boldsymbol{\eta}} + \mathbf{J}^{-1}\mathbf{G}(\boldsymbol{\eta}) \end{aligned},$$

$\mathbf{M}_{\eta}(\boldsymbol{\eta}) = \mathbf{J}^{-\mathrm{T}}(\boldsymbol{\eta})\mathbf{M}\mathbf{J}^{-1}(\boldsymbol{\eta})$, $\mathbf{b}_{\boldsymbol{\eta}} = \mathbf{J}^{-\mathrm{T}}(\boldsymbol{\eta})\Delta f$. $\mathbf{u} = \mathbf{J}^{-\mathrm{T}}(\boldsymbol{\eta})\boldsymbol{\tau} = \mathbf{J}(\boldsymbol{\eta})\boldsymbol{\tau}$

Let $\mathbf{M}_{\boldsymbol{\eta}}^{-1}(\mathbf{y}) = \mathrm{g}(\mathbf{y}) + \mathrm{g}_{\Delta}(\mathbf{y})$, where $\mathrm{g}(\mathbf{y})$ includes the diagonal elements of $\mathbf{M}_{\boldsymbol{\eta}}^{-1}(\mathbf{y})$, and $\mathrm{g}_{\Delta}(\mathbf{y})$ is the non-diagonal elements of $\mathbf{M}_{\boldsymbol{\eta}}^{-1}(\mathbf{y})$. So the equation (9) can be rewritten as:

$$\begin{cases} \ddot{y}_i = f_i(\mathrm{x}) + \mathrm{g}_{ii}(\mathrm{x})u_i + d_{si} \\ d_{si} = \sum\limits_{j=1, j\neq i}^{n}\mathrm{g}_{ij}(\mathrm{x})u_j + d_i \end{cases} \quad i = 1,\cdots 6 \tag{10}$$

where u_i is the main input value for the i-th sub-system, d_{si} means the equivalent disturbance of the i-th sub-system. So the

MIMO system is divided into six SISO systems. Assume that the equivalent disturbance of the i-th sub-system is bounded, i.e. $\|d_{si}\| \le D_{si}$, and g_0 is the lower bound of $\mathrm{g}_{ii}(\mathrm{x}), i = 1,2\cdots 6$, i.e. $\mathrm{g}_{ii}(\mathrm{x}) \ge \mathrm{g}_0 > 0$.

D. Control objective

Define the constant vector $\mathbf{y}_d = [y_{d1},...,y_{dn}]^{\mathrm{T}}$ as the desired output value of the system. To make the differential of $\mathbf{y}_d$ meaningful always and improve the tracking performance, a smooth reference trajectory $\mathbf{y}_{ref} = \left[y_{ref1},...,y_{refn}\right]^{\mathrm{T}}$ for the tracking system will be generated by the pre-filter:

$$\mathbf{M}_r\ddot{\mathbf{y}}_{ref} + \mathbf{D}_r\dot{\mathbf{y}}_{ref} + \mathbf{G}_r\mathbf{y}_{ref} = \mathbf{G}_r\mathbf{y}_d \tag{11}$$

where $\mathbf{M}_r$, $\mathbf{D}_r$, and $\mathbf{G}_r$ are positive design matrices.

The control objective is to devise a neural network-based adaptive output feedback controller $\mathbf{u}$, such that the output signals $\mathbf{y}$ follows a desired reference trajectory $\mathbf{y}_{ref}$, and the signals in the closed-loop system are stay bounded.

III. CONTROLLER DESIGN

In this section, an RWNN-based adaptive robust controller is employed for AUV's positioning system.

Considering the i-th sub-system (5), defining the extensional error:

$$s_i = \dot{e}_i + \lambda e_i \tag{12}$$

where $e_i = y_{refi} - y_i$ is the tracking error of the i-th subsystem, so the s_i dynamics can be described as:

$$\begin{aligned}\dot{s}_i &= \ddot{e}_i + \lambda\dot{e}_i \\ &= \ddot{y}_{refi} - \ddot{y}_i + \lambda\dot{e}_i \\ &= \ddot{y}_{refi} + \lambda\dot{e}_i - f_i(\mathrm{x}) - \mathrm{g}_{ii}(\mathrm{x})\tau_i - d_{si} \\ &= -\mathrm{g}_{ii}(\mathrm{x})\tau_i + a_i(\dot{y}_{refi},\ddot{y}_{refi}) + b_i(\mathrm{x},\dot{y}_i) - d_{si}\end{aligned} \tag{13}$$

where $a_i(\dot{y}_{refi},\ddot{y}_{refi}) = \ddot{y}_{refi} + \lambda\dot{y}_{refi}$, $b_i(\mathrm{x},\dot{y}_i) = -f_i(\mathrm{x}) + \lambda\dot{y}_i$.

A. Controller design without disturbances

An ideal controller is derived in this section for the s_i dynamics under the assumption $d_{si} = 0$:

$$\begin{gathered}u_i^* = \lambda K_i e_i + \frac{1}{g_{ii}(\mathrm{x})}(\overline{a}_i(y_{refi},\dot{y}_{refi},\ddot{y}_{refi}) + \overline{b}_i(\mathrm{x},y_i,\dot{y}_i)) \\ i = 1,2\cdots n\end{gathered} \tag{14}$$

where $\overline{a}_i(y_{refi},\dot{y}_{refi},\ddot{y}_{refi}) = a_i(\dot{y}_{refi},\ddot{y}_{refi}) + g_{ii}(\mathrm{x})\mathrm{k}_i\,\dot{y}_{refi}$, and $\overline{b}_i(\mathrm{x},y_i,\dot{y}_i) = b_i(\mathrm{x},\dot{y}_i) - g_{ii}(\mathrm{x})\mathrm{k}_i\,\dot{y}_i$. K_i>0 is a feedback gain and the extensional error s_i will be converge to zero.

Proof Considering the Lyapunov function candidate as follows:

$$V = \frac{1}{2}s_i^{\,2} \tag{15}$$

So the derivative of the function (15) along the trajectory as:

$$\begin{aligned}\dot{V} &= s_i\dot{s}_i \\ &= -\mathrm{g}_{ii}(\mathrm{x})K_i s_i(\dot{y}_{refi} - \dot{y}_i + \lambda e_i) \\ &= -\mathrm{g}_{ii}(\mathrm{x})K_i s^2_{\ i} \le 0\end{aligned} \tag{16}$$

then we have the asymptotic result $\lim\limits_{x\to\infty} s_i = 0$.

We notice that the controller (14) is especially idealistic. Let:

$$u_{1i}^* = \frac{1}{g_{ii}(\mathrm{x})}(\overline{a}_i(y_{refi},\dot{y}_{refi},\ddot{y}_{refi}) + \overline{b}_i(\mathrm{x},y_i,\dot{y}_i)) \tag{17}$$

Considering the ideal controller, we notice that u_1^* includes the vehicle parameters, which is hard to obtain in practical solution. Especially for the 6 DOF underwater vehicles, it is often impractical to get all the values in the system matrix and the modelling error cannot be ignored too. For these reasons, a recurrent wavelet neural network is employed to approximate the unknown function u_1^*, and the controller can be rewritten as:

$$u_i = \lambda K_i e_i + \hat{u}_{1i} + \hat{u}_{si} \tag{18}$$

where $\hat{u}_1$ is the output of RWNN, which will be designed later. $\hat{u}_r$ is the robust controller, which is used to handle the disturbances and the approximate error of the neural network.

B. Recurrent wavelet neural network

RWNN is a dynamic recurrent multilayered network with memory elements and an internal feedback loop, and it can captures the dynamic response of a system. The derivatives $\dot{\mathbf{y}}$ which cannot be obtain directly will not be used as one of the input vector. A MIMO RWNN's structure are introduced as follows, see Fig. 2.

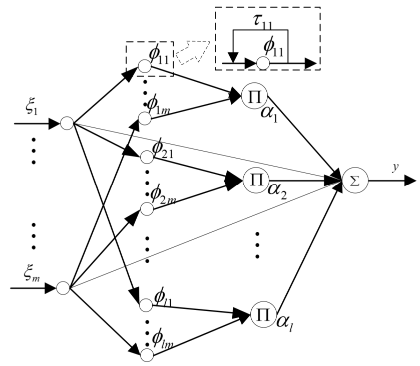

Fig. 2. the structure of RWNN

The RWNN comprises input layer, mother wavelet layer, product layer and output layer. For the m inputs and one output neural network model, there are l nodes in product layer, so The number of mother wavelet layer nodes is $m \times l$. Because of the feedback construct in the mother wavelet layer and the differential relation between the signals, we can choose $\mathbf{y}_i$ and $\mathbf{y}_{refi}$ as the inputs of the RWNN to approximate the unknown function in (8). So the input vector can be chosen as $\boldsymbol{\xi} = \begin{bmatrix} \mathbf{y}^T & \mathbf{y}_{ref}{}^T \end{bmatrix}^T \in \Re^m$. Select $\phi(x) = -x \exp((-1/2)x^2)$ as the mother wavelet function, which has the universal approximation property, so the output of product layer can be obtain through:

$$\begin{aligned}\alpha_j &= \prod_{k=1}^{m} \phi_{jk} = \prod_{k=1}^{m} \phi_{jk} \left(\frac{\xi_k + \phi_{jk}(t-\Delta t) r_{jk} - \mu_{jk}}{d_{jk}}\right) \\ &= \prod_{k=1}^{m} \left(\frac{\xi_k + \phi_{jk}(t-\Delta t) r_{jk} - \mu_{jk}}{d_{jk}}\right) \\ &\quad \times \exp\left(\frac{(\xi_k + \phi_{jk}(t-\Delta t) r_{jk} - \mu_{jk})^2}{2 d_{jk}{}^2}\right) \\ &\qquad (k = 1, 2 \cdots m; j = 1, 2 \cdots l)\end{aligned} \tag{19}$$

where r_{jk} is the recurrent weight of the mother wavelet node. $\phi_{jk}(t-\Delta t)$ represents the output of mother wavelet node through delay time Δt. μ_{jk} is the translation factor and d_{jk} is the dilation factor. It can be seen that mother wavelet layer accepts not only the outputs of layer 1 but also the feedback values through delay.

Then the output of the RWNN can be written as:

$$y_{RWNN}(\boldsymbol{\xi}, \boldsymbol{\mu}, \mathbf{d}, \mathbf{r}, \mathbf{W}, \boldsymbol{\Theta}) = \mathbf{W}^{\mathbf{T}} \boldsymbol{\alpha}(\boldsymbol{\xi}, \boldsymbol{\mu}, \mathbf{d}, \mathbf{r}) + \boldsymbol{\Theta}^{\mathbf{T}} \boldsymbol{\xi} \tag{20}$$

where $\mathbf{W} = [w_1, w_2, \cdots w_l]^T \in \Re^l$, and w_j is the connection weight value between j-th product node and i-th output node. $\boldsymbol{\Theta} = [\theta_1, \theta_2, \cdots \theta_m]^T \in \Re^m$ is the connection weight vector between the input nodes and the output nodes. $\boldsymbol{\alpha}(\boldsymbol{\xi}, \boldsymbol{\mu}, \mathbf{d}, \mathbf{r})$ represents the outputs of the product layer. Define the matrices $\boldsymbol{\mu}$, $\mathbf{d}$, $\mathbf{r}$ as:

$$\boldsymbol{\mu} = [\boldsymbol{\mu}_1^T, \cdots \boldsymbol{\mu}_j^T, \cdots \boldsymbol{\mu}_l^T]^T , \quad \boldsymbol{\mu}_j = [\mu_{j1}, \mu_{j2}, \cdots \mu_{jm}]^T \in \Re^m ,$$
$$\mathbf{d} = [\mathbf{d}_1^T, \cdots \mathbf{d}_j^T, \cdots \mathbf{d}_l^T]^T , \quad \mathbf{d}_j = [d_{j1}, d_{j2}, \cdots d_{jm}]^T \in \Re^m ,$$
$$\mathbf{r} = [\mathbf{r}_1^T, \cdots \mathbf{r}_j^T, \cdots \mathbf{r}_l^T]^T , \quad \mathbf{r}_j = [r_{j1}, r_{j2}, \cdots r_{jm}]^T \in \Re^m .$$

According to the approximation theorem, there exist matrixes $\mathbf{W}^*$, $\boldsymbol{\Theta}^*$, $\boldsymbol{\mu}^*$, $\mathbf{d}^*$, $\mathbf{r}^*$, such that the continuous function on a compact set can be approximated by recurrent wavelet the neural work, i.e.

$$u_{1i}^* = \frac{\overline{\alpha}_i + \overline{\beta}_i}{g_{ii}(x)} = \mathbf{W}^{*\mathbf{T}} \boldsymbol{\alpha}(\boldsymbol{\xi}, \boldsymbol{\mu}^*, \mathbf{d}^*, \mathbf{r}^*) + \boldsymbol{\Theta}^{*\mathbf{T}} \boldsymbol{\xi} + \varepsilon \tag{21}$$

where ε is the reconstruction error of the neural network, and $\|\varepsilon\| < \varepsilon_N$, ε_N is the upper bound of ε . Since the optimal values cannot be obtain in practical application, we use $\hat{\mathbf{W}}$, $\hat{\boldsymbol{\Theta}}$, $\hat{\boldsymbol{\mu}}$, $\hat{\mathbf{d}}$, $\hat{\mathbf{r}}$ as the estimation of the optimal values, and they will be used in the final controller, i.e.

$$\hat{u}_{1i} = \hat{\mathbf{W}}^{\mathbf{T}} \boldsymbol{\alpha}(\boldsymbol{\xi}, \hat{\boldsymbol{\mu}}, \hat{\mathbf{d}}, \hat{\mathbf{r}}) + \hat{\boldsymbol{\Theta}}^{\mathbf{T}} \boldsymbol{\xi} \tag{22}$$

Adaptation laws and robust controller design

Define the estimation error vectors

$$\begin{aligned}\tilde{\mathbf{W}} &= \mathbf{W}^* - \hat{\mathbf{W}} \\ \tilde{\boldsymbol{\mu}} &= \boldsymbol{\mu}^* - \hat{\boldsymbol{\mu}} \\ \tilde{\mathbf{d}} &= \mathbf{d}^* - \hat{\mathbf{d}} \\ \tilde{\boldsymbol{\Theta}} &= \boldsymbol{\Theta}^* - \hat{\boldsymbol{\Theta}}\end{aligned} \tag{23}$$

and

$$\tilde{\boldsymbol{\alpha}} = \boldsymbol{\alpha}(\boldsymbol{\xi}, \boldsymbol{\mu}^*, \mathbf{d}^*, \mathbf{r}^*) - \boldsymbol{\alpha}(\boldsymbol{\xi}, \hat{\boldsymbol{\mu}}, \hat{\mathbf{d}}, \hat{\mathbf{r}}) \tag{24}$$

So the estimation error of the RWNN can be written as

$$\begin{aligned}\tilde{u}_{1i} &= u_{1i}^* - \hat{u}_{1i} \\ &= \mathbf{W}^{*\mathbf{T}} \boldsymbol{\alpha}^* + \boldsymbol{\Theta}^{*\mathbf{T}} \boldsymbol{\xi} - \hat{\mathbf{W}}^{\mathbf{T}} \hat{\boldsymbol{\alpha}} - \hat{\boldsymbol{\Theta}}^{\mathbf{T}} \boldsymbol{\xi} + \varepsilon \\ &= \hat{\mathbf{W}}^{\mathbf{T}} \tilde{\boldsymbol{\alpha}} + \tilde{\mathbf{W}}^{\mathbf{T}} \boldsymbol{\alpha}^* + \tilde{\boldsymbol{\Theta}}^{\mathbf{T}} \boldsymbol{\xi} + \varepsilon\end{aligned} \tag{25}$$

Moreover, the Taylor series is employed to transform $\tilde{\boldsymbol{\alpha}}$ into a partially linear form, i.e.

$$\begin{aligned}\tilde{\boldsymbol{\alpha}} &= \frac{\partial \boldsymbol{\alpha}}{\partial \boldsymbol{\mu}^T}\Big|_{\boldsymbol{\mu}=\hat{\boldsymbol{\mu}}} \tilde{\boldsymbol{\mu}} + \frac{\partial \boldsymbol{\alpha}}{\partial \mathbf{d}^T}\Big|_{\mathbf{d}=\hat{\mathbf{d}}} \tilde{\mathbf{d}} + \frac{\partial \boldsymbol{\alpha}}{\partial \mathbf{r}^T}\Big|_{\mathbf{r}=\hat{\mathbf{r}}} \tilde{\mathbf{r}} \\ &\quad + o(\tilde{\mathbf{d}}^2) + o(\tilde{\boldsymbol{\mu}}^2) + o(\tilde{\mathbf{r}}^2)\end{aligned} \tag{26}$$

where $o(\tilde{\mathbf{d}}^2)$, $o(\tilde{\boldsymbol{\mu}}^2)$, $o(\tilde{\mathbf{r}}^2)$ are the high order terms. For convenience, Let

$$\hat{\boldsymbol{\alpha}}_{\boldsymbol{\mu}} = \frac{\partial \boldsymbol{\alpha}}{\partial \boldsymbol{\mu}^T}\Big|_{\boldsymbol{\mu}=\hat{\boldsymbol{\mu}}},\ \hat{\boldsymbol{\alpha}}_{\mathbf{d}} = \frac{\partial \boldsymbol{\alpha}}{\partial \mathbf{d}^T}\Big|_{\mathbf{d}=\hat{\mathbf{d}}},\ \hat{\boldsymbol{\alpha}}_{\mathbf{r}} = \frac{\partial \boldsymbol{\alpha}}{\partial \mathbf{r}^T}\Big|_{\mathbf{r}=\hat{\mathbf{r}}}. \tag{27}$$

So the estimation error $\tilde{u}_{ri}$ can be rewritten as

$$\begin{aligned}\tilde{u}_{ri} &= \hat{\mathbf{W}}^{\mathbf{T}}\tilde{\boldsymbol{\alpha}} + \tilde{\mathbf{W}}^{\mathbf{T}}\boldsymbol{\alpha}^* + \tilde{\boldsymbol{\Theta}}^{\mathbf{T}}\boldsymbol{\xi} + \varepsilon \\ &= \tilde{\mathbf{W}}^{\mathbf{T}}(\hat{\boldsymbol{\alpha}} + \hat{\boldsymbol{\alpha}}_{\boldsymbol{\mu}}\tilde{\boldsymbol{\mu}} + \hat{\boldsymbol{\alpha}}_{\mathbf{d}}\tilde{\mathbf{d}} + \hat{\boldsymbol{\alpha}}_{\mathbf{r}}\tilde{\mathbf{r}}) + \hat{\mathbf{W}}^{\mathbf{T}}(\hat{\boldsymbol{\alpha}}_{\boldsymbol{\mu}}\tilde{\boldsymbol{\mu}} + \hat{\boldsymbol{\alpha}}_{\mathbf{d}}\tilde{\mathbf{d}} + \hat{\boldsymbol{\alpha}}_{\mathbf{r}}\tilde{\mathbf{r}}) \\ &\quad \mathbf{W}^{*\mathbf{T}}(o(\tilde{\mathbf{d}}^2) + o(\tilde{\boldsymbol{\mu}}^2) + o(\tilde{\mathbf{r}}^2)) + \tilde{\boldsymbol{\Theta}}^{\mathbf{T}}\boldsymbol{\xi} + \varepsilon \\ &= \tilde{\mathbf{W}}^{\mathbf{T}}(\hat{\boldsymbol{\alpha}} - \hat{\boldsymbol{\alpha}}_{\boldsymbol{\mu}}\hat{\boldsymbol{\mu}} - \hat{\boldsymbol{\alpha}}_{\mathbf{d}}\hat{\mathbf{d}} - \hat{\boldsymbol{\alpha}}_{\mathbf{r}}\hat{\mathbf{r}}) + \tilde{\boldsymbol{\mu}}^{\mathbf{T}}\hat{\boldsymbol{\alpha}}_{\boldsymbol{\mu}}^{\mathbf{T}}\hat{\mathbf{W}} \\ &\quad + \tilde{\mathbf{d}}^{\mathbf{T}}\hat{\boldsymbol{\alpha}}_{\mathbf{d}}^{\mathbf{T}}\hat{\mathbf{W}} + \tilde{\mathbf{r}}^{\mathbf{T}}\hat{\boldsymbol{\alpha}}_{\mathbf{r}}^{\mathbf{T}}\hat{\mathbf{W}} + \tilde{\boldsymbol{\Theta}}^{\mathbf{T}}\boldsymbol{\xi} + h\end{aligned} \tag{28}$$

where

$$h = \tilde{\mathbf{W}}^{\mathbf{T}}(\hat{\boldsymbol{\alpha}}_{\boldsymbol{\mu}}\boldsymbol{\mu}^* + \hat{\boldsymbol{\alpha}}_{\mathbf{d}}\mathbf{d}^* + \hat{\boldsymbol{\alpha}}_{\mathbf{r}}\mathbf{r}^*) + \mathbf{W}^{*\mathbf{T}}(o(\tilde{\mathbf{d}}^2) + o(\tilde{\boldsymbol{\mu}}^2) + o(\tilde{\mathbf{r}}^2)) + \varepsilon$$

For the i-th sub-system, the adaptive laws is defined as follows

$$\dot{\hat{\mathbf{W}}} = \gamma_1(s_i(\hat{\boldsymbol{\alpha}} - \hat{\boldsymbol{\alpha}}_{\boldsymbol{\mu}}\hat{\boldsymbol{\mu}} - \hat{\boldsymbol{\alpha}}_{\mathbf{d}}\hat{\mathbf{d}} - \hat{\boldsymbol{\alpha}}_{\mathbf{r}}\hat{\mathbf{r}}) - \sigma_1|s_i|\hat{\mathbf{W}}) \tag{29}$$

$$\dot{\hat{\boldsymbol{\Theta}}} = \gamma_2(s_i\xi - \sigma_2|s_i|\hat{\boldsymbol{\Theta}}) \tag{30}$$

$$\dot{\hat{\boldsymbol{\mu}}} = \gamma_3(\hat{\boldsymbol{\alpha}}_{\boldsymbol{\mu}}^{\mathbf{T}}s_i\hat{\mathbf{W}} - \sigma_3|s_i|\hat{\boldsymbol{\mu}}) \tag{31}$$

$$\dot{\hat{\mathbf{d}}} = \gamma_4(\hat{\boldsymbol{\alpha}}_{\mathbf{d}}^{\mathbf{T}}s_i\hat{\mathbf{W}} - \sigma_4|s_i|\hat{\mathbf{d}}) \tag{32}$$

$$\dot{\hat{\mathbf{r}}} = \gamma_5(\hat{\boldsymbol{\alpha}}_{\mathbf{r}}^{\mathbf{T}}s_i\hat{\mathbf{W}} - \sigma_5|s_i|\hat{\mathbf{r}}) \tag{33}$$

where $\gamma_1,\gamma_2,\gamma_3,\gamma_4,\gamma_5 > 0$, $\sigma_1,\sigma_2,\sigma_3,\sigma_4,\sigma_5 > 0$ are adaptive gain.

Let

$$\rho = \sigma_1\|\mathbf{W}^*\|^2 + \sigma_2\|\boldsymbol{\Theta}^*\|^2 + \sigma_3\|\boldsymbol{\mu}^*\|^2 + \sigma_4\|\mathbf{d}^*\|^2 + \sigma_5\|\mathbf{r}^*\|^2 \tag{34}$$

$$\Delta_i = h_i + \rho + \frac{1}{\mathrm{g}_0}D_{si} \tag{35}$$

A robust controller can be chosen as follows to balance the approximation error of the neural network and the disturbances in the system.

$$\dot{\hat{\Delta}}_i = \gamma_6|s_i| \tag{36}$$

$$\dot{\delta}_i = -\gamma_6\frac{|s_i|\hat{\Delta}_i}{|s_i|^2 + \delta_i} \tag{37}$$

$$u_{si} = \frac{s_i|s_i|\hat{\Delta}_i}{|s_i|^2 + \delta_i} \tag{38}$$

The control law is design as(18), which is comprised of a RWNN and a robust controller, and the parameter adaptive laws are chosen as (29)-(33). The robust controller is designed as (38), and the parameters are adjusted by (36)-(37), the asymptotic stability can be guaranteed.

C. Stability analysis

Considering the s_i system

$$\begin{aligned}\dot{s}_i &= -\mathrm{g}_{ii}(\mathrm{x})u_i + \alpha_i + \beta_i - d_{si} \\ &= -\mathrm{g}_{ii}(\mathrm{x})u_i + \alpha_i - \mathrm{g}_{ii}(\mathrm{x})\frac{\overline{\alpha}_i + \overline{\beta}_i}{\mathrm{g}_{ii}(\mathrm{x})} + \mathrm{g}_{ii}(\mathrm{x})u_{1i}^* + \beta_i - d_{si} \\ &= -\mathrm{g}_{ii}(\mathrm{x})\lambda K_i s_i + \mathrm{g}_{ii}(\mathrm{x})(\tilde{u}_{1i} - u_{si}) - d_{si} \\ &= -\mathrm{g}_{ii}(\mathrm{x})\lambda K_i s_i + \mathrm{g}_{ii}(\mathrm{x})(\tilde{\mathbf{W}}^{\mathbf{T}}(\hat{\boldsymbol{\alpha}} - \hat{\boldsymbol{\alpha}}_{\boldsymbol{\mu}}\hat{\boldsymbol{\mu}} - \hat{\boldsymbol{\alpha}}_{\mathbf{d}}\hat{\mathbf{d}} - \hat{\boldsymbol{\alpha}}_{\mathbf{r}}\hat{\mathbf{r}}) \\ &\quad + \tilde{\boldsymbol{\mu}}^{\mathbf{T}}\hat{\boldsymbol{\alpha}}_{\boldsymbol{\mu}}^{\mathbf{T}}\hat{\mathbf{W}} + \tilde{\mathbf{d}}^{\mathbf{T}}\hat{\boldsymbol{\alpha}}_{\mathbf{d}}^{\mathbf{T}}\hat{\mathbf{W}} + \tilde{\mathbf{r}}^{\mathbf{T}}\hat{\boldsymbol{\alpha}}_{\mathbf{r}}^{\mathbf{T}}\hat{\mathbf{W}} + \tilde{\boldsymbol{\Theta}}^{\mathbf{T}}\boldsymbol{\xi} + h_i - u_{si}) - d_{si}\end{aligned} \tag{39}$$

A Lyapunov function can be chosen as follows:

$$\begin{aligned}V &= \frac{1}{2}s_i^2 + \mathrm{g}_{ii}(\mathrm{x})(\frac{1}{2\gamma_1}\tilde{\mathbf{W}}^{\mathbf{T}}\tilde{\mathbf{W}} + \frac{1}{2\gamma_2}\tilde{\boldsymbol{\Theta}}^{\mathbf{T}}\tilde{\boldsymbol{\Theta}} + \frac{1}{2\gamma_3}\tilde{\boldsymbol{\mu}}^{\mathbf{T}}\tilde{\boldsymbol{\mu}} \\ &\quad + \frac{1}{2\gamma_4}\tilde{\mathbf{d}}^{\mathbf{T}}\tilde{\mathbf{d}} + \frac{1}{2\gamma_5}\tilde{\mathbf{r}}^{\mathbf{T}}\tilde{\mathbf{r}} + \frac{1}{2\gamma_6}\tilde{\Delta}_i^2 + \frac{1}{2\gamma_6}\delta_i^2)\end{aligned} \tag{40}$$

where $\tilde{\Delta}_i = \Delta_i - \hat{\Delta}_i$. Taking the time derivative of the Lyapunov function, yield

$$\begin{aligned}\dot{V} &= s_i\dot{s}_i - \mathrm{g}_{ii}(\mathrm{x})(\frac{1}{\gamma_1}\tilde{\mathbf{W}}^{\mathbf{T}}\dot{\hat{\mathbf{W}}} + \frac{1}{\gamma_2}\tilde{\boldsymbol{\Theta}}^{\mathbf{T}}\dot{\hat{\boldsymbol{\Theta}}} + \frac{1}{\gamma_3}\tilde{\boldsymbol{\mu}}^{\mathbf{T}}\dot{\hat{\boldsymbol{\mu}}} + \frac{1}{\gamma_4}\tilde{\mathbf{d}}^{\mathbf{T}}\dot{\hat{\mathbf{d}}} \\ &\quad + \frac{1}{\gamma_5}\tilde{\mathbf{r}}^{\mathbf{T}}\dot{\hat{\mathbf{r}}} + \frac{1}{\gamma_6}\tilde{\Delta}_i\dot{\hat{\Delta}}_i - \frac{1}{\gamma_6}\delta_i\dot{\delta}_i) \\ &= -\mathrm{g}_{ii}(\mathrm{x})\lambda K_i s_i^2 + \mathrm{g}_{ii}(\mathrm{x})s_i(\tilde{\mathbf{W}}^{\mathbf{T}}(\hat{\boldsymbol{\alpha}} - \hat{\boldsymbol{\alpha}}_{\boldsymbol{\mu}}\hat{\boldsymbol{\mu}} - \hat{\boldsymbol{\alpha}}_{\mathbf{d}}\hat{\mathbf{d}} - \hat{\boldsymbol{\alpha}}_{\mathbf{r}}\hat{\mathbf{r}}) \\ &\quad + \tilde{\boldsymbol{\mu}}^{\mathbf{T}}\hat{\boldsymbol{\alpha}}_{\boldsymbol{\mu}}^{\mathbf{T}}\hat{\mathbf{W}} + \tilde{\mathbf{d}}^{\mathbf{T}}\hat{\boldsymbol{\alpha}}_{\mathbf{d}}^{\mathbf{T}}\hat{\mathbf{W}} + \tilde{\mathbf{r}}^{\mathbf{T}}\hat{\boldsymbol{\alpha}}_{\mathbf{r}}^{\mathbf{T}}\hat{\mathbf{W}} + \tilde{\boldsymbol{\Theta}}^{\mathbf{T}}\boldsymbol{\xi}) \\ &\quad + \mathrm{g}_{ii}(\mathrm{x})s_i(h_i - u_{si} - \frac{1}{\mathrm{g}_{ii}(\mathrm{x})}d_{si}) - \mathrm{g}_{ii}(\mathrm{x})(\frac{1}{\gamma_1}\tilde{\mathbf{W}}^{\mathbf{T}}\dot{\hat{\mathbf{W}}} + \frac{1}{\gamma_2}\tilde{\boldsymbol{\Theta}}^{\mathbf{T}}\dot{\hat{\boldsymbol{\Theta}}} \\ &\quad + \frac{1}{\gamma_3}\tilde{\boldsymbol{\mu}}^{\mathbf{T}}\dot{\hat{\boldsymbol{\mu}}} + \frac{1}{\gamma_4}\tilde{\mathbf{d}}^{\mathbf{T}}\dot{\hat{\mathbf{d}}} + \frac{1}{\gamma_5}\tilde{\mathbf{r}}^{\mathbf{T}}\dot{\hat{\mathbf{r}}} + \frac{1}{\gamma_6}\tilde{\Delta}_i\dot{\hat{\Delta}}_i - \frac{1}{\gamma_6}\delta_i\dot{\delta}_i)\end{aligned} \tag{41}$$

Since there is a inequality as follows

$$\begin{aligned}\tilde{\mathbf{W}}^{\mathbf{T}}\hat{\mathbf{W}} &\le \tilde{\mathbf{W}}^{\mathbf{T}}(\mathbf{W}^* - \tilde{\mathbf{W}}) \\ &\le \tilde{\mathbf{W}}^{\mathbf{T}}\mathbf{W}^* - \|\tilde{\mathbf{W}}\|^2 \le -\frac{1}{2}\|\tilde{\mathbf{W}}\|^2 + \|\mathbf{W}^*\|^2\end{aligned} \tag{42}$$

And in a similar way, we have

$$\tilde{\boldsymbol{\Theta}}^{\mathbf{T}}\hat{\boldsymbol{\Theta}} \le -\frac{1}{2}\left\|\tilde{\boldsymbol{\Theta}}\right\|^2 + \left\|\boldsymbol{\Theta}^*\right\|^2 \tag{43}$$

$$\tilde{\boldsymbol{\mu}}^{\mathbf{T}}\hat{\boldsymbol{\mu}} \le -\frac{1}{2}\left\|\tilde{\boldsymbol{\mu}}\right\|^2 + \left\|\boldsymbol{\mu}^*\right\|^2 \tag{44}$$

$$\tilde{\mathbf{d}}^{\mathbf{T}}\hat{\mathbf{d}} \le -\frac{1}{2}\left\|\tilde{\mathbf{d}}\right\|^2 + \left\|\mathbf{d}^*\right\|^2 \tag{45}$$

$$\tilde{\mathbf{r}}^{\mathbf{T}}\hat{\mathbf{r}} \le -\frac{1}{2}\left\|\tilde{\mathbf{r}}\right\|^2 + \left\|\mathbf{r}^*\right\|^2 \tag{46}$$

Substitute equation (37-41) into equation (36), Yield

$$\begin{aligned}
\dot{V} &\le -\mathrm{g}_{ii}(\mathrm{x})\lambda K_i s_i^2 - \mathrm{g}_{ii}(\mathrm{x})\left(\frac{1}{\gamma_6}\tilde{\Delta}_i\dot{\hat{\Delta}}_i - \frac{1}{\gamma_6}\delta_i\dot{\delta}_i\right) \\
&\quad + \mathrm{g}_{ii}(\mathrm{x})s_i\left(h_i - \frac{s_i\left|s_i\right|\hat{\Delta}_i}{\left|s_i\right|^2+\delta_i} + \frac{1}{\mathrm{g}_0}D_{si}\right) + \mathrm{g}_{ii}(\mathrm{x})\left|s_i\right|\rho \\
&\quad -\frac{1}{2}\mathrm{g}_{ii}(\mathrm{x})\left|s_i\right|\left(\sigma_1\left\|\tilde{\mathbf{W}}\right\|^2 + \sigma_2\left\|\tilde{\boldsymbol{\Theta}}\right\|^2 + \sigma_3\left\|\tilde{\boldsymbol{\mu}}\right\|^2 + \sigma_4\left\|\tilde{\mathbf{d}}\right\|^2 + \sigma_5\left\|\tilde{\mathbf{r}}\right\|^2\right) \\
&\le -\mathrm{g}_{ii}(\mathrm{x})\lambda K_i s_i^2 - \mathrm{g}_{ii}(\mathrm{x})\left(\frac{1}{\gamma_6}\tilde{\Delta}_i\dot{\hat{\Delta}}_i - \frac{1}{\gamma_6}\delta_i\dot{\delta}_i\right) \\
&\quad + \mathrm{g}_{ii}(\mathrm{x})\left(\Delta_i s_i - \frac{s_i^2\left|s_i\right|\hat{\Delta}_i}{\left|s_i\right|^2+\delta_i}\right) \\
&\quad -\frac{1}{2}\mathrm{g}_{ii}(\mathrm{x})\left|s_i\right|\left(\sigma_1\left\|\tilde{\mathbf{W}}\right\|^2 + \sigma_2\left\|\tilde{\boldsymbol{\Theta}}\right\|^2 + \sigma_3\left\|\tilde{\boldsymbol{\mu}}\right\|^2 + \sigma_4\left\|\tilde{\mathbf{d}}\right\|^2 + \sigma_5\left\|\tilde{\mathbf{r}}\right\|^2\right)
\end{aligned} \tag{47}$$

Yield

$$\begin{aligned}
\dot{V} &\le -\mathrm{g}_{ii}(\mathrm{x})\lambda K_i s_i^2 + \mathrm{g}_{ii}(\mathrm{x})\left(\tilde{\Delta}_i\left|s_i\right| + \delta_i\frac{s_i\hat{\Delta}_i}{\left|s_i\right|^2+\delta_i}\right) \\
&\quad - \mathrm{g}_{ii}(\mathrm{x})\left(\frac{1}{\gamma_6}\tilde{\Delta}_i\dot{\hat{\Delta}}_i - \frac{1}{\gamma_6}\delta_i\dot{\delta}_i\right) \\
&\quad -\frac{1}{2}\mathrm{g}_{ii}(\mathrm{x})\left|s_i\right|\left(\sigma_1\left\|\tilde{\mathbf{W}}\right\|^2 + \sigma_2\left\|\tilde{\boldsymbol{\Theta}}\right\|^2 + \sigma_3\left\|\tilde{\boldsymbol{\mu}}\right\|^2 + \sigma_4\left\|\tilde{\mathbf{d}}\right\|^2 + \sigma_5\left\|\tilde{\mathbf{r}}\right\|^2\right) \\
&\le -\mathrm{g}_{ii}(\mathrm{x})\lambda K_i s_i^2 \\
&\quad -\frac{1}{2}\mathrm{g}_{ii}(\mathrm{x})\left|s_i\right|\left(\sigma_1\left\|\tilde{\mathbf{W}}\right\|^2 + \sigma_2\left\|\tilde{\boldsymbol{\Theta}}\right\|^2 + \sigma_3\left\|\tilde{\boldsymbol{\mu}}\right\|^2 + \sigma_4\left\|\tilde{\mathbf{d}}\right\|^2 + \sigma_5\left\|\tilde{\mathbf{r}}\right\|^2\right)
\end{aligned} \tag{48}$$

From the inequality of $\dot{V}$ given by (42), we can see that $\dot{V}$ is a negative semi-definite function, i.e. $\dot{V} \le 0$. It implies that s_i, $\tilde{\mathbf{W}}$, $\tilde{\boldsymbol{\Theta}}$, $\tilde{\boldsymbol{\mu}}$, $\tilde{\mathbf{d}}$, $\tilde{\mathbf{r}}$, $\tilde{\Delta}_i$, δ_i are bounded. Since V is a non-increasing and bounded function, and we have $\lim_{t\to\infty} V(\mathrm{t}) = V(\infty)$. So :

$$\begin{aligned}
&\int_0^\infty \left(\mathrm{g}_{ii}(\mathrm{x})\lambda K_i z_i^2 + \frac{1}{2}\mathrm{g}_{ii}(\mathrm{x})\left|z_i\right|\left(\sigma_1\left\|\tilde{\mathbf{W}}\right\|^2 + \sigma_2\left\|\tilde{\boldsymbol{\Theta}}\right\|^2 + \sigma_3\left\|\tilde{\boldsymbol{\mu}}\right\|^2\right.\right. \\
&\left.\left. + \sigma_4\left\|\tilde{\mathbf{d}}\right\|^2 + \sigma_5\left\|\tilde{\mathbf{r}}\right\|^2\right)\right) \le V(0) - V(\infty) < \infty
\end{aligned} \tag{49}$$

Since the function $\mathrm{g}_{ii}(\mathrm{x})\lambda K_i s_i^2 + \frac{1}{2}\mathrm{g}_{ii}(\mathrm{x})\left|s_i\right|\rho$ is bounded, according to Barbalat's Lemma, the convergence can be guaranteed, i.e. $\mathrm{g}_{ii}(\mathrm{x})\lambda K_i s_i^2 + \frac{1}{2}\mathrm{g}_{ii}(\mathrm{x})\left|s_i\right|\rho \to 0$, when $t \to \infty$. Furthermore, it implies that $\left|s_i\right|$ converge to zero as $t \to \infty$.

IV. CASE STUDY

To validate the proposed RWNN-based robust adaptive controller, it is assessed in the MATLAB simulation environment with a six DOF nonlinear model of an underwater vehicle. The initial position of the ROV is $\mathbf{y} = [\ -85\ 0\ 47.5\ 0\ 0\ 0]^T$, and the desired position and attitude is $\mathbf{y}_d = [\ -80\ 2\ 50\ 5\ 5\ 5]^T$.

The pre-filter is utilizing to produce a smooth target path for the controller, and the parameter matrixes can be chosen as:

$$\begin{aligned}
\mathbf{M}_r &= diag([1,1,1,1,1,1]) \\
\mathbf{D}_r &= 2\mathbf{M}_r\boldsymbol{\xi}\boldsymbol{\Omega} \\
\mathbf{G}_r &= \mathbf{M}_r\boldsymbol{\Omega}^2 \\
\boldsymbol{\xi} &= diag([3,3,3,3,3,3]) \\
\boldsymbol{\Omega} &= diag([2,2,2,2,2,2])
\end{aligned}$$

A RWNN which has 6 nodes in the product layer is used in the control system, the input vector of the neural network is $\boldsymbol{\xi} = \left[\mathbf{y}^T \quad \mathbf{y}_{ref}{}^T\right]^T$, and the parameters of the weight updating laws are chosen as: $\gamma_1 = \gamma_2 = \gamma_3 = \gamma_4 = \gamma_5 = 20$; $\sigma_1 = \sigma_2 = \sigma_3 = \sigma_4 = \sigma_5 = 6.2$.

The robust controller's parameters are chosen as $\gamma_6 = 0.1$. The initial values of $\hat{\Delta}$ is zero, and the initial values of δ is 0.5.

To verify the effectiveness of the controller and the control effect, the unpredictable disturbances and parameter uncertainties are introduced. The environmental disturbances acting on the underwater vehicle and the uncertainties of the model can be treated together as:

$$\Delta f = [1000, 1000, 500, 1000, 1000, 1000]^{\mathrm{T}}$$

The 3D trajectory of the vehicle with umbilical cable is shown in Fig.3, it is indicate that the proposed controller can drive the vehicle from the initial position to the given position $\mathbf{y}_d$. The lines stand for the cable's configuration at different time.

Fig. 4 shows the curves of vehicles' position and attitude, the dotted lines present the output of the pre-filter, and solid lines are the time history of $x, y, z, \phi, \theta, \psi$. From the curves, it is shown that the output of the vehicle can follow the reference trajectory well.

Fig. 5 shows the time history of error function s . From the figure, we can see that the error function s get to zero at 10-15s by using the proposed controller.

Fig. 6 shows the curves of control inputs by using the proposed method. In general, the better tracking precision needs more control effort and may cause oscillations of the control. As seen from Fig. 8, there are few slight oscillations at the beginning because of the existence of the RWNN, but the outputs of the thruster are smooth and steady. In addition, since the given signals which the controller need are given by the pre-filter, so the errors are changing smooth and slowly, and it causing that the magnitude of the thruster are never get the maximum values.

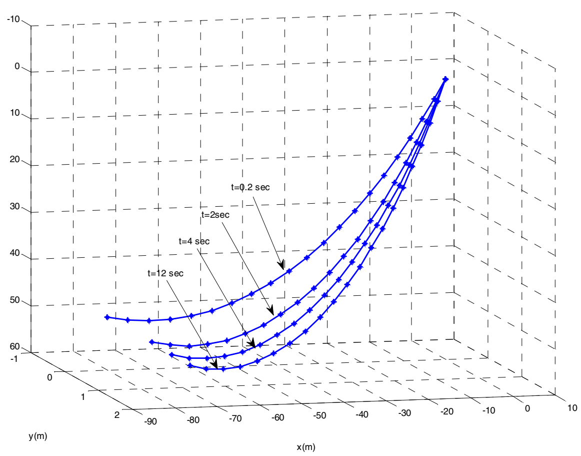

Fig. 3. The trajectory of the ROV with umbilical cable

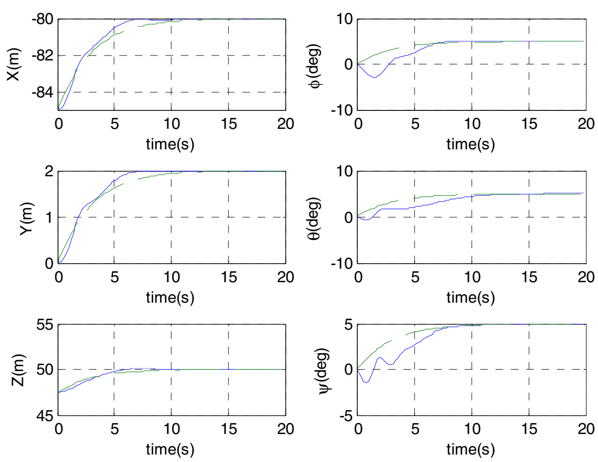

Fig. 4. The time history of the undetwater vehicle

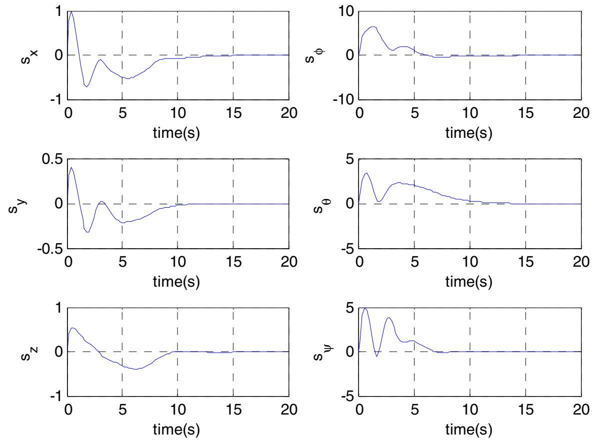

Fig. 5. The time history of the extensional error function s

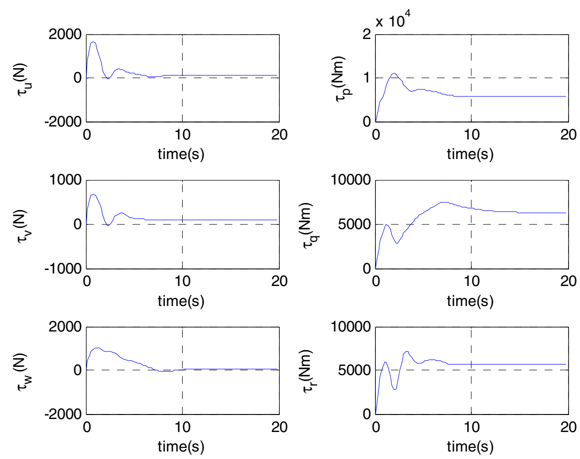

Fig. 6. Control input using the proposed controller

V. Conclusions

In this paper, the problem of station keeping for a ROV with parameter uncertainties and unknown external disturbances has been investigated. Firstly, the MIMO system was divided into several SISO systems by a transformation. So the output of the system is decoupled with the control input. Then, A RWNN is used to approach the unknown term in the ideal controller, and a special robust controller is designed to compensate the approximate error and the equivalent error. Stability analysis is made to verify the asymptotically stable of the final closed-loop system. The tracking error can convergence to zero. The excellent performance of the aforementioned control scheme is validated through simulation for the station keeping of an underwater vehicle

Conflict of Interests

The authors declare that there is no conflict of interests regarding the publication of this paper.

REFERENCES

[1] Conrado de Souza, E., Maruyama, N., Intelligent UUVs: Some Issues on ROV Dynamic Positioning. IEEE Transactions on Aerospace and Electronic Systems. 2007, 43 (1), pp. 214-226.

[2] Savaresi, S.M., Previdi, F., Alessandro, D., Sergio B., et al. Modeling, Identification, and Analysis of Limit-Cycling Pitch and Heave Dynamics in ROV. IEEE Journal of Oceanic Engineering. 2004, 29, pp. 407-417.

[3] Fossen T I. Handbook of marine craft hydrodynamics and motion control [M]. John Wiley & Sons, 2011.

[4] G. Zhang, L. Yu, X. Meng, L. Zhang, Tracking control of underactuated ship based on partial state feedback scheme.In: Proceedings of 2011 IEEE/ICME International Conference on Complex Medical ngineering, pp. 678-683, 2011.

[5] Nambisan P R, Singh S N. Multi-variable adaptive back-stepping control of submersibles using SDU decomposition[J]. Ocean Engineering, 2009, 36(2): 158-167.

[6] Li, J. H., Lee, P. M.. Design of an adaptive nonlinear controller for depth control of an autonomous underwater vehicle. Ocean Engineering. 2005, 32(18), pp. 2165-2181.

[7] Wu, T. Z., Juang, Y.T.. Adaptive fuzzy sliding-mode controller of uncertain nonlinear systems, ISA Transactions. 2008, 47(3), pp. 279-285.

[8] H. Nguyen quang, E. Kreuzer, (2007). Adaptive PD-controller for positioning of a remotely operated vehicle close to an underwater structure: Theory and experiments. Control Engineering Practice, 411-419.

[9] Zhu K.W., Gu L.Y.. A MIMO nonlinear robust controller for work-class ROVs positioning and trajectory tracking control. In: 2011 Chinese Control and Decision Conference. 2011, pp.2565-2570.

[10] Ishaque K, Abdullah S S, Ayob S M, et al. Single input fuzzy logic controller for unmanned underwater vehicle[J]. Journal of Intelligent and Robotic Systems, 2010, 59(1): 87-100.

[11] Ishaque K, Abdullah S S, Ayob S M, et al. A simplified approach to design fuzzy logic controller for an underwater vehicle[J]. Ocean Engineering, 2011, 38(1): 271-284.

[12] Pan C Z, Yang S X, Lai X Z, et al. An efficient neural network based tracking controller for autonomous underwater vehicles subject to unknown dynamics[C]//Control and Decision Conference (2014 CCDC), The 26th Chinese. IEEE, 2014: 3300-3305.

[13] J. H. Li, P. M. Lee, A neural network adaptive controller design for free-pitch-angle diving behavior of an autonomous underwater vehicle[J]. Robotics and Autonomous Systems, 2005, 52(2): 132-147.

[14] Zhang L J, Qi X, Pang Y J. Adaptive output feedback control based on DRFNN for AUV[J]. Ocean Engineering, 2009, 36(9): 716-722.

[15] C. H, Chen, C. F. Hsu, Recurrent wavelet neural backstepping controller design with a smooth compensator[J]. Neural Computing and Applications, 2010, 19(7): 1089-1100.

[16] C. H, Chen, Wavelet-based adaptive robust control for a class of MIMO uncertain nonlinear systems[J]. Neural Computing and Applications, 2012, 21(4): 747-762.

[17] Z.Feng, R.Allen, Evaluation of the effects of the communication cable on the dynamic of an underwater flight vehicle, Ocean Engineering. 31(2004) 1019-1035.

[18] Fang M C, Hou C S, Luo J H. On the motions of the underwater remotely operated vehicle with the umbilical cable effect[J]. Ocean engineering, 2007, 34(8): 1275-1289.